CWP-465
November 2003

Application of PS-wave moveout asymmetry in parameter estimation for tilted TI media

Pawan Dewangan and Ilya Tsvankin

Center for Wave Phenomena
Department of Geophysics
Colorado School of Mines
Golden, Colorado 80401
(303)273-3557

ABSTRACT

One of the distinctive features of mode-converted waves is their asymmetric moveout (i.e., PS-wave traveltime may not stay the same if the source and receiver are interchanged) caused by lateral heterogeneity or elastic anisotropy. If the medium is anisotropic, the moveout asymmetry contains valuable information for parameter estimation that cannot be obtained from pure reflection modes.

Here, we generalize the so-called "PP+PS=SS" method, which is designed to replace reflected PS modes in velocity analysis with pure (non-converted) SS-waves, by supplementing the output SS traces with the moveout asymmetry attributes of PS-waves. The moveout asymmetry factor Δt_{PS} is computed in the slowness domain as the difference between the traveltimes of the PS arrivals with opposite signs of the ray parameter (horizontal slowness). Another useful asymmetry attribute is the offset $x_{\min}(\alpha)$ of the PS-wave moveout minimum on a common-midpoint (CMP) gather with azimuth α. The computation of both Δt_{PS} and $x_{\min}$ is integrated in a straighforward way into the processing flow of the PP+PS=SS method.

The effectiveness of the developed algorithm and the importance of including the asymmetry attributes of PS-waves in anisotropic velocity analysis are demonstrated for transversely isotropic models with a tilted symmetry axis (TTI media). Simple analytic expressions for the moveout asymmetry of the PSV-wave in a horizontal TTI layer are derived in the weak-anisotropy approximation and verified by anisotropic ray tracing. The asymmetry attributes reach their maximum in the vertical plane that contains the symmetry axis and vanish in the orthogonal direction. The factor Δt_{PS} is proportional to the anellipticity parameter η and rapidly varies with the tilt ν of the symmetry axis. The largest values of Δt_{PS} are found for the symmetry axis that deviates by 20-30° from the vertical or horizontal directions.

All relevant parameters of a TTI layer can be estimated by a nonlinear inversion of the normal-moveout (NMO) velocities and zero-offset traveltimes of PP- and SS(actually, SVSV)-waves combined with the moveout asymmetry attributes of the PSV-wave. It should be emphasized that the inversion of pure-mode (PP and SS) moveouts alone is ambiguous, while the addition of the attributes Δt_{PS} and $x_{\min}$ yields stable parameter estimates for noise-contaminated input data. Although the algorithm generally requires a wide range of azimuths, the parameters of most TTI models (except those with near-horizontal axis orientations) can be obtained from 2-D data acquired in the vertical symmetry-axis plane. If the TTI model is formed by obliquely dipping fractures, the estimated anisotropic parameters can be inverted further for the fracture orientation and compliances.

INTRODUCTION

The complex, multidimensional nature of inverse problems in anisotropic media makes it imperative to combine different wave types in estimating medium parameters. In particular, building anisotropic models for depth imaging usually requires supplementing P-waves with mode conversions or S-waves (e.g., Tsvankin, 2001). Since excitation of shear waves is still relatively rare, most multicomponent data sets include P-waves and converted PS-waves. Although the benefits of using PS-waves in various applications are well documented in the literature (e.g., Thomsen, 1999), processing of mode conversions is complicated by several factors related to the asymmetry of their raypath (e.g., Grechka and Tsvankin, 2002).

The difficulties in adjusting seismic processing algorithms for PS data prompted Grechka and Tsvankin (2002) and Grechka and Dewangan (2003) to develop the so-called "PP+PS=SS" method designed to construct "quasi-SS" reflections[1] from PP and PS data without precise knowledge of the velocity model. The moveout of the original PP arrivals can then be combined with that of the computed SS-waves in anisotropic stacking-velocity tomography (Grechka et al., 2002a) or other velocity-analysis algorithms. This approach significantly simplifies the inversion/processing flow for multicomponent surveys, and it proved to be effective in anisotropic velocity analysis of field data (Grechka et al., 2002b).

While replacing PS-waves with pure SS reflections is advantageous from the processing viewpoint, the PP+PS=SS method does not preserve the information about the asymmetry of PS moveout. If the medium is either laterally heterogeneous or anisotropic without a horizontal symmetry plane, the traveltime of PS-waves does not remain the same when the source and receiver are interchanged (Pelissier et al., 1991; Thomsen, 1999; Tsvankin and Grechka, 2000). This moveout asymmetry of PS reflections was shown by Tsvankin and Grechka (2000, 2002) to provide critically important attributes for parameter estimation in transversely isotropic media with a vertical symmetry axis (VTI). In the PP+PS=SS method (Grechka and Tsvankin, 2002a), however, the traveltime of the constructed SS arrival for each source-receiver pair is obtained from the *sum* of the "reciprocal" PS-wave times corresponding to same reflection point. (By "reciprocal" times we mean the times of the PS-waves that have the same absolute value but opposite signs of the projection of the slowness vector onto the reflector.) As a result, the *difference* between the reciprocal times that quantifies the moveout asymmetry does not contribute to the computed SS data and cannot be used in the subsequent velocity analysis.

This paper demonstrates that supplementing the output of the PP+PS=SS method (i.e., PP and SS data) with the moveout asymmetry attributes of PS-waves can help to build an anisotropic velocity field in the depth domain without *a priori* information. We consider the model of a transversely isotropic layer with a tilted symmetry

[1]The constructed SS events have the correct kinematics, but not the amplitudes, of the SS-wave primary reflections.

axis (TTI) that describes, for example, obliquely dipping, rotationally invariant fractures embedded in isotropic host rock. Other examples of subsurface TTI formations include progradational clastic or carbonate sequences (e.g., Sarg and Schuelke, 2003) and dipping shale layers in fold-and-thrust belts (e.g., in the Canadian Foothills) and near salt domes. The TTI medium is parameterized here by the velocities of P- and S-waves in the symmetry direction (V_{P0} and V_{S0}, respectively), the tilt of the symmetry axis from the vertical (ν) and Thomsen's (1986) anisotropic coefficients ϵ, δ, and γ defined in the coordinate system associated with the symmetry axis (Tsvankin, 2001).

In principle, the symmetry-axis orientation and the parameters V_{P0}, ϵ, and δ can be estimated from P-wave data alone, but this inversion requires the normal-moveout (NMO) ellipses (i.e., wide-azimuth P-wave reflections) from a horizontal and a dipping interface, and both the tilt ν and reflector dip should be no less than 30–40° (Grechka and Tsvankin, 2000). Although the addition of the NMO ellipses of pure SV-waves to those of P-waves makes it possible to invert for the TTI parameters using the reflections from a single interface, the parameter estimation is still ambiguous for a range of small tilts and reflector dips (Grechka and Tsvankin, 2000; Grechka et al., 2002a). Therefore, even the wide-azimuth traveltimes of pure reflection modes (P and SV) from subhorizontal interfaces are insufficient for reconstructing the TTI model.

The asymmetry of PS moveout in TTI media is caused by the tilt of the symmetry axis, which creates a model without a horizontal symmetry plane. The possibility of using traveltime asymmetry information in estimating the parameters of a fractured TTI layer was demonstrated on field data by Angerer et al. (2002). Here, we present an analytic study of the PSV-wave moveout asymmery in a horizontal TTI layer and develop an inversion algorithm that operates with both pure and converted reflection modes. Numerical tests on noise-contaminated data indicate that the inversion is sufficiently stable if the symmetry axis deviates from the vertical by 10° or more. The instability of the parameter estimation for subvertical symmetry-axis orientation is expected because for VTI media even long-spread (nonhyperbolic) moveout of PP- and PSV-waves does not constrain the parameters V_{P0}, V_{S0}, ϵ, and δ (Grechka and Tsvankin, 2002b).

MODIFICATION OF THE PP+PS=SS METHOD

The PP+PS=SS method introduced by Grechka and Tsvankin (2002a) is designed for seismic surveys in which shear waves are not excited (e.g., ocean-bottom cable, or OBC) but may be recorded by multicomponent receivers. In this case, the shear wavefield is formed by mode-converted PS-waves, with the conversion often happening at the reflector. Although PS arrivals carry valuable information about the shear-wave velocities, inversion and processing of mode conversions is hindered by their large reflection-point dispersal, polarity reversals, and moveout asymmetry. The idea of the PP+PS=SS method is to recompute the recorded PP and PS wavefields into the corresponding pure SS reflections, which are not physically generated in the survey.

The construction of SS-waves with the correct kinematics (but not amplitudes) does not require explicit information about the velocity field, but it is necessary to correlate PP and PS arrivals and identify the events reflected from the same interface. The original version of the PP+PS=SS method described by Grechka and Tsvankin (2002a) operates with PP and PS traveltimes picked on prestack data. As illustrated in Figure 1, matching the reflection slopes on common-receiver gathers makes it possible to find two PS rays (recorded at points $x^{(3)}$ and $x^{(4)}$) with the same reflection point as the PP reflection $x^{(1)}Rx^{(2)}$. Then the traveltime of the SS-wave is determined from

$$\tau_{SS}(x^{(3)}, x^{(4)}) = t_{PS}(x^{(1)}, x^{(3)}) + t_{PS}(x^{(2)}, x^{(4)}) - t_{PP}(x^{(1)}, x^{(2)}). \qquad (1)$$

Application of equation (1) produces reflection SS data with the correct kinematics but generally distorted amplitudes. Clearly, the SS traveltime $\tau_{SS}(x^{(3)}, x^{(4)})$ will remain the same if we interchange the source ($x^{(3)}$) and receiver ($x^{(4)}$). Therefore, the moveout of the constructed SS-waves in common-midpoint (CMP) geometry is always symmetric, as is the case for any pure reflection mode. Conventional-spread SS traveltimes are described by the NMO velocity (in 2-D) and NMO ellipse (in 3-D), which can be obtained using algorithms developed for PP-wave data. The NMO velocities or ellipses of the PP- and SS-waves can then be combined in velocity analysis using, for example, stacking-velocity tomography, which proved to be particularly efficient for anisotropic media (Grechka et al., 2002a).

Still, for many anisotropic models including a horizontal TTI layer, pure reflection modes are not sufficient for estimating the vertical velocities and anisotropic coefficients (Grechka and Tsvankin, 2000; Grechka et al., 2002a). In such a case, an important question is whether or not including some attributes of the recorded PS-waves in the inversion algorithm can help in recovering the medium parameters. It is clear from equation (1) that the information about the moveout asymmetry of PS arrivals is not preserved in the computed SS traveltime, which depends on only the *sum* of the traveltimes of the PS-waves converted at point R (Figure 1). Below, we add certain measures of the PS-wave moveout asymmetry to the traveltimes of the PP-waves and the reconstructed SS-waves in the inversion for the parameters of TTI media.

A generalized version of the PP+PS=SS method based on equation (1) was developed by Grechka and Dewangan (2003). Instead of operating with prestack PP and PS traveltimes, they apply a particular convolution of PP and PS traces to produce seismograms of the corresponding SS-waves. The convolution operator in the frequency domain is given by

$$W_{SS}(\omega, x^{(3)}, x^{(4)}) = \iint \Big[\quad W_{PS}(\omega, x^{(1)}, x^{(3)})\, W^{*}_{PP}(\omega, x^{(1)}, x^{(2)}) \times \\ W_{PS}(\omega, x^{(2)}, x^{(4)}) \Big]\, dx^{(1)}\, dx^{(2)}, \qquad (2)$$

where ω is the radial frequency, W_{PP} are W_{PS} are the spectra of PP and PS traces,

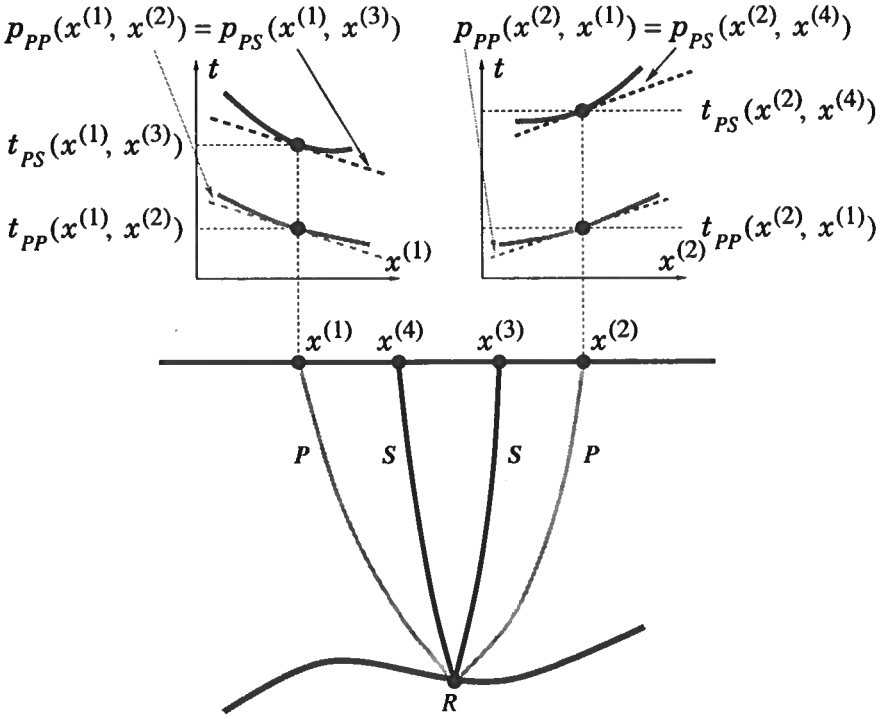

FIG. 1. 2-D ray diagram of the PP+PS=SS method (after Grechka and Tsvankin, 2002a). The reflected PP ray from $x^{(1)}$ to $x^{(2)}$ and the PS rays from $x^{(1)}$ to $x^{(3)}$ and $x^{(2)}$ to $x^{(4)}$ have the same reflection point R. The rays with the common reflection point are identified by matching the slopes on common-receiver gathers (i.e., the ray parameters) of the PP- and PS-waves.

W_{SS} is the spectrum of the constructed SS trace for the source and receiver located at points $x^{(3)}$ and $x^{(4)}$, and the star denotes complex conjugate. The integration is performed over the P-wave source and receiver coordinates $x^{(1)}$ and $x^{(2)}$ (Figure 1). The main contribution to the integral comes from the stationary point that yields the traveltime of the constructed SS-wave given by equation (1):

$$\tau_{SS}(x^{(3)}, x^{(4)}) = \min_{x^{(1)},\, x^{(2)}} \left(t_{PS}(x^{(1)}, x^{(3)}) + t_{PS}(x^{(2)}, x^{(4)}) - t_{PP}(x^{(1)}, x^{(2)}) \right). \quad (3)$$

To preserve information about the moveout asymmetry of the recorded PS-wave, we suggest to generate an *asymmetry gather* in addition to the SS data. When using the PP+PS=SS method, it is natural to define the asymmetry through the difference between the two PS traveltimes corresponding to the same reflection point (Figure 1):

$$\Delta t_{PS}(x^{(3)}, x^{(4)}) = t_{PS}(x^{(1)}, x^{(3)}) - t_{PS}(x^{(2)}, x^{(4)}). \quad (4)$$

We modified the algorithm of Dewangan and Grechka (2003) to estimate the stationary points given by equation (3). Then the difference between the PS traveltimes (picked on the original data) corresponding to each stationary point is used to compute the asymmetry factor from equation (4).

If the reflector is horizontal and the overburden is laterally homogeneous, the two reciprocal PS-waves in Figure 1 have the same magnitude but opposite signs of the ray parameter (horizontal slowness) – that of the PP reflection from $x^{(1)}$ to $x^{(2)}$. Hence, equation (4) defines the asymmetry of the PS moveout in the slowness domain. Analytic expressions that describe the asymmetry factor Δt_{PS} are given in the next section.

Integral (2) can be extended to 3-D multiazimuth reflection data. Since sources and receivers then cover an area on the earth's surface, their coordinates $\boldsymbol{x}$ become two-component vectors. The integration then has to be performed over four coordinates, and the stationary point [equation (3)] corresponds to a minimum in the 4-D space.

ASYMMETRIC MOVEOUT OF PS-WAVES IN TTI MEDIA

Parametric moveout equations

Consider a PS-wave formed by mode conversion at an interface underlying an arbitrarily anisotropic, homogeneous layer. In general, an incident P-wave in such a model excites two reflected shear modes (PS_1 and PS_2). The traveltime of either PS-wave can be represented in parametric form as (Tsvankin and Grechka, 2002)

$$t_{PS} \equiv t_P + t_S = z\,(q_P - p_{1P}\,q_{,1P} - p_{2P}\,q_{,2P} + q_S - p_{1S}\,q_{,1S} - p_{2S}\,q_{,2S}), \quad (5)$$

where t_P and t_S are the traveltimes along the P- and S-legs, respectively, z is the depth of the reflection (conversion) point, p_1 and p_2 are the horizontal components of

the slowness vector (the subscripts "P" and "S" indicate the wave type), $q \equiv p_3$ is the vertical slowness, and $q_{,i} \equiv \partial q/\partial p_i$ $(i = 1, 2)$ (Figure A-1). Following Tsvankin and Grechka (2002), the slownesses are computed under the convention that the x_3-axis points up, and both legs of the PS ray represent upgoing waves (i.e., the corresponding group-velocity vectors point toward the earth's surface).

Here, we study a horizontal layer, in which the projections of the slowness vectors of the P- and S-legs onto the horizontal plane have to be identical to comply with Snell's law:

$$p_{1P} = -p_{1S} \equiv p_1\,; \quad p_{2P} = -p_{2S} \equiv p_2. \tag{6}$$

Equation (5) then simplifies to

$$t_{PS} = z\left[q_P + q_S - p_1\left(q_{,1P} - q_{,1S}\right) - p_2\left(q_{,2P} - q_{,2S}\right)\right]. \tag{7}$$

The corresponding source-receiver vector $\boldsymbol{x}$ of PS-waves in an anisotropic, homogeneous layer can be also expressed through the slowness components (Tsvankin and Grechka, 2002):

$$\boldsymbol{x}_{PS} = \{x_1, x_2\} = z\left\{\left(q_{,1P} - q_{,1S}\right), \left(q_{,2P} - q_{,2S}\right)\right\}; \tag{8}$$

$$x_1 = q_{,1P} - q_{,1S}\,,$$

$$x_2 = q_{,2P} - q_{,2S}\,.$$

Equation (8) yields the source-receiver offset x and the azimuth α of the source-receiver line with respect to the x_1-axis:

$$x_{PS} = |\boldsymbol{x}_{PS}| = \sqrt{x_1^2 + x_2^2}\,, \tag{9}$$

$$\alpha = \tan^{-1}\left(\frac{x_2}{x_1}\right). \tag{10}$$

Moveout asymmetry in the slowness domain

For laterally homogeneous models, such as a horizontal TTI layer treated below, the moveout of converted waves becomes asymmetric only if the medium does not have a horizontal symmetry plane (e.g., Tsvankin, 2001). Conventionally, the moveout asymmetry is estimated in the offset domain by interchanging the source and receiver positions. Here, however, we define the traveltime asymmetry factor in the slowness domain:

$$\Delta t_{PS} = t_{PS}(p_1, p_2) - t_{PS}(-p_1, -p_2) = \Delta t_P + \Delta t_S, \tag{11}$$

where Δt_P and Δt_S represent the contributions to Δt_{PS} from the P- and S-legs of the PS ray, respectively. Equation (11) describes the difference between the traveltimes of the PS arrivals excited by incident P-waves that have the same magnitude but opposite signs of the horizontal projection of the slowness vector.

If the moveout of PS-waves is symmetric, then changing the sign of the horizontal slowness reverses the direction of the source-receiver vector $\boldsymbol{x}$ [equation (8)] with no change in the absolute value of offset. Hence, the measure of asymmetry for $\boldsymbol{x}$ can be defined in the following way:

$$\Delta \boldsymbol{x}_{PS} = \boldsymbol{x}_{PS}(p_1, p_2) + \boldsymbol{x}_{PS}(-p_1, -p_2)\,. \tag{12}$$

The main advantage of treating the asymmetry in the slowness domain is that, for a laterally homogeneous medium, both Δt_{PS} and $\Delta \boldsymbol{x}_{PS}$ can be obtained directly from the PP+PS=SS method [see equation (4) and Figure 1]. Equations (7), (11), (8), and (12) give an exact representation of the moveout asymmetry of PS-waves for any horizontal anisotropic layer. Next, we apply this formulation to study the dependence of Δt_{PS} on the parameters of TI media with an arbitrary tilt of the symmetry axis. The factor $\Delta \boldsymbol{x}_{PS}$ is discussed later on, after the introduction of the offset $x_{\min}$ of the PS-wave moveout minimum in CMP geometry.

Since the contributions of the symmetry-axis orientation and anisotropic parameters to the time asymmetry factor Δt_{PS} are hidden in the components of the slowness vector, in Appendix A we linearize equation (11) with respect to ϵ and δ under the assumption of weak anisotropy ($|\epsilon| \ll 1$ and $|\delta| \ll 1$). The derivation is carried out for the PS mode that is polarized in the plane formed by the slowness vector and the symmetry axis. Note that although we will denote this wave "PSV," its polarization vector lies in the vertical incidence plane only if that plane contains the symmetry axis.

The coordinate system is chosen in such a way that the symmetry axis is confined to the $[x_1, x_3]$-plane, which represents the only vertical symmetry plane of the model and will be called here the *symmetry-axis plane* (Figure A-1). The sign of the time difference in equation (11) is specified by assuming that the symmetry axis is dipping in the positive x_1-direction.

Substituting equations (A-5) and (A-6) into equation (11), we obtain a linearized expression for the moveout asymmetry factor of the PSV-wave:

$$\Delta t_{PS} = -8\,\eta\, z\, V_{P0}^2\, p_1\, [p_2^2 + (2p_1^2 + p_2^2)\cos 2\nu]\, \sin 2\nu\,, \tag{13}$$

where $\eta \equiv (\epsilon - \delta)/(1 + 2\delta) \approx \epsilon - \delta$ is the "anellipticity" coefficient responsible for time processing of P-wave data in VTI media (Alkhalifah and Tsvankin, 1995). In the symmetry-axis plane $[x_1, x_3]$, the slowness component p_2 vanishes that and equation (13) simplifies to

$$\Delta t_{PS}(p_2 = x_2 = 0) = -8\,\eta\, z\, V_{P0}^2\, p_1^3\, \sin 4\nu\,. \tag{14}$$

Equations (13) and (14) give a concise description of the azimuthally-varying factor Δt_{PS}. The main properties of the PSV-wave moveout asymmetry in the slowness domain can be summarized as follows:

- The asymmetry factor vanishes for VTI ($\nu = 0°$) and HTI ($\nu = 90°$) media because these two models have a horizontal symmetry plane. In the symmetry-axis plane, the linearized factor Δt_{PS} [equation (14)] also goes to zero for $\nu = 45°$. In this case, however, the higher-order terms in ϵ and δ do not vanish, which makes the moveout weakly asymmetric.

- The contributions to the asymmetry factor from the P-leg [equation (A-5)] and S-leg [equation (A-6)] of the converted wave are identical. Although this result was proved here in the weak-anisotropy approximation, numerical tests show that it remains valid for arbitrary strength of the anisotropy.

- The asymmetry in the slowness domain depends only on the *difference* $\eta = \epsilon - \delta$ and vanishes if the anisotropy is elliptical ($\epsilon = \delta$). Since for elliptical media with any magnitude of $\epsilon = \delta$ there is no SV-wave velocity anisotropy, the S-leg of the converted wave does not produce any moveout asymmetry. This means that the P-leg cannot cause the asymmetry either (see above).

- The magnitude of the asymmetry factor in the symmetry-axis plane [equation (14)] reaches its maximum for the tilts $\nu = 22.5°$ and $\nu = 67.5°$. Therefore, Δt_{PS} is quite sensitive to the deviation of the symmetry axis from the vertical and horizontal directions.

The azimuthally-varying asymmetry factor Δt_{PS} computed for a typical TTI model from the exact equations (7) and (11) is displayed in Figure 2. There is a substantial variation of Δt_{PS} with the slowness component p_1 (e.g., in the x_1-direction where $p_2 = 0$), while the influence of p_2 is much weaker. Therefore, Figure 2 indicates that most of the 3-D (wide-azimuth) moveout asymmetry information can be obtained in the symmetry-axis plane $[x_1, x_3]$.

Note that the line $p_1 = 0$ in Figure 2 where $\Delta t_{PS} = 0$ *does not* correspond to acquisition in the $[x_2, x_3]$-plane. Since $[x_2, x_3]$ is not a symmetry plane, downgoing P rays with $p_1 = 0$ deviate from the vertical incidence plane $[x_2, x_3]$, and the source-receiver direction of the reflected PS-wave is not parallel to the x_2-axis.

Figure 3 shows the function $\Delta t_{PS}(p_1)$ in the symmetry-axis plane in more detail. Both the PP+PS=SS method and parametric equation (11) are supposed to produce exact values of Δt_{PS}, which is confirmed by our numerical results. The magnitude of the asymmetry factor is quite substantial – it exceeds 40% of the zero-offset time before rapidly decreasing for large values of p_1.

The accuracy of the weak-anisotropy approximation (14) in Figure 3 is quite satisfactory considering that it incorporates the contribution of the S-leg of the converted wave. Typically, the weak-anisotropy approximation is much less accurate for SV-waves than it is for P-waves because of the large magnitude of the anisotropic parameter $\sigma \equiv (V_{P0}^2/V_{S0}^2)(\epsilon - \delta)$ (Tsvankin and Thomsen, 1994; Tsvankin, 2001). In our case, however, the anisotropy-related asymmetry factors for the P- and S-legs are

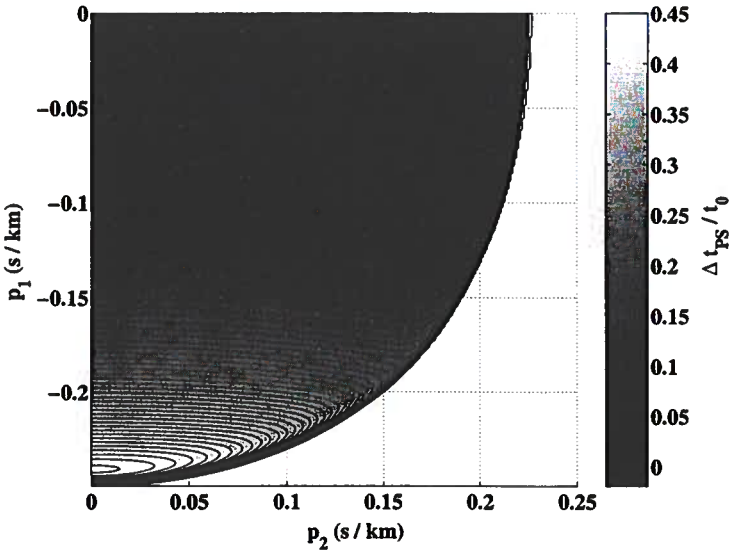

FIG. 2. Exact asymmetry factor Δt_{PS} in the slowness domain for the PSV-wave in a horizontal TTI layer. Δt_{PS} is normalized by the zero-offset traveltime t_0 of the PS-wave. The asymmetry for negative slowness p_2 is not shown because $\Delta t_{PS}(p_1, -p_2) = \Delta t_{PS}(p_1, p_2)$. The medium parameters are $V_{P0} = 4$ km/s, $V_{S0} = 2$ km/s, $\epsilon = 0.1$, $\delta = -0.1$, $\nu = 70°$, and $z = 1$ km.

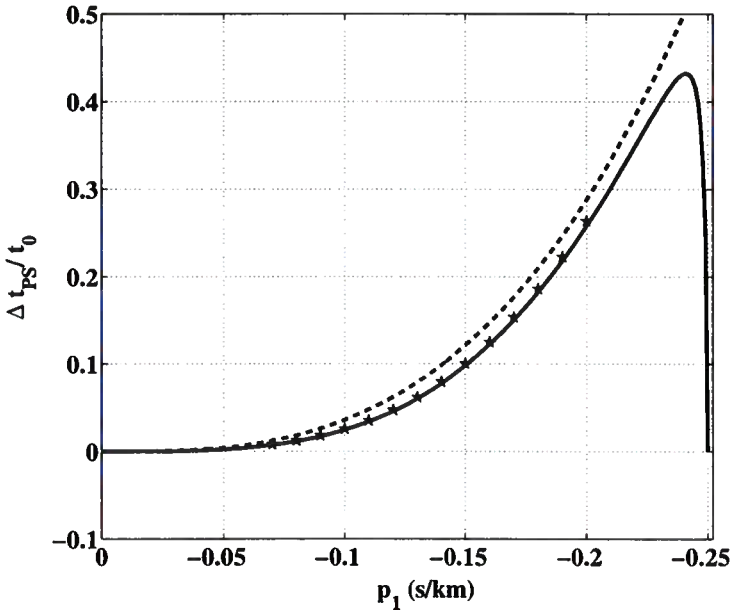

FIG. 3. Asymmetry factor from Figure 2 in the $[x_1, x_3]$-plane. The solid line is obtained from the exact parametric equation (11); the dashed line is the weak-anisotropy approximation (14). The stars denote the output (represented as a function of p_1) of the PP+PS = SS method; the maximum offset-to-depth ratio of the PP and PS data is close to two.

equal to each other (see above), and the error of the weak-anisotropy approximation is the same for both P- and S-waves.

Moveout asymmetry in the offset domain

Most existing results on the moveout asymmetry of PS-waves are obtained in the offset domain (Thomsen, 1999; Tsvankin and Grechka, 2000, 2002). If the source and receiver positions are interchanged, the traveltime of the converted wave does not remain the same unless the reflector is horizontal and the medium above it is laterally homogeneous and has a horizontal symmetry plane. For PS data collected in a common-midpoint (CMP) gather centered at the origin of the coordinate system, the asymmetry factor in the offset domain is defined as

$$\Delta t_{PS} = t_{PS}(\boldsymbol{x}_{PS}) - t_{PS}(-\boldsymbol{x}_{PS}), \tag{15}$$

where $\boldsymbol{x}_{PS}$ is the offset vector of the PS-wave given by equation (8).

Azimuthally varying minimum-time offset $\boldsymbol{x}_{\min}$.—If reflection moveout is asymmetric, the minimum of the traveltime curve in a common-midpoint gather is shifted from the CMP location. The offset corresponding to the traveltime minimum (we denote it by $x_{\min}$) is a convenient measure of the asymmetry that depends on the reflector orientation and anisotropic parameters. Analytic expressions for $x_{\min}$ in a VTI layer above a dipping reflector are given by Tsvankin and Grechka (2000, 2002) and Tsvankin (2001). In a horizontal TTI layer, $x_{\min}$ carries useful information about the tilt of the symmetry axis and the anisotropic parameters.

In Appendix B we use equations (8)–(10) for the offset $\boldsymbol{x}$ in terms of the ray parameter to obtain the following simple expression for the azimuthal variation of $x_{\min}$:

$$x_{\min}(\alpha) = x_0 \cos\alpha, \tag{16}$$

where $x_0 = x_{\min}(\alpha = 0°)$ is the offset of the traveltime minimum in the symmetry-axis plane $[x_1, x_3]$ given in equation (B-5):

$$x_0 = x_{\min}(\alpha = 0°) = z \left[\epsilon \sin 2\nu - \frac{\eta}{2}\left(1 + \frac{V_{P0}^2}{V_{S0}^2}\right) \sin 4\nu\right]. \tag{17}$$

According to equation (16), $x_{\min}(\alpha)$ reaches its maximum in the symmetry-axis plane and vanishes in the orthogonal direction. If $x_{\min}$ is plotted as the radius vector for each azimuth α, it should trace out a circle with radius $x_0/2$ and center $(x_0, 0)$ on the x_1-axis.

While equation (17) for x_0 is valid only in the weak-anisotropy limit, the azimuthal dependence of $x_{\min}$ is described by equation (16) for any strength of the anisotropy. Figure 4 demonstrates that for the model used in the previous section, values of $x_{\min}(\alpha)$ obtained from anisotropic ray tracing lie on the circle computed

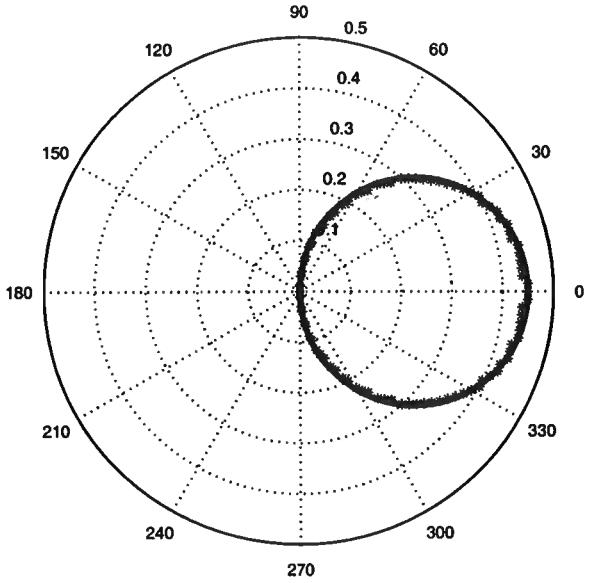

FIG. 4. Polar plot of the offset $x_{\min}(\alpha)$ for the model from Figure 2. The stars mark values obtained from anisotropic ray tracing of PS-waves and the solid line is computed from equation (16) with the exact value of x_0.

from equation (16) with the exact x_0. Similar results were obtained for TTI models with much larger magnitudes of the anisotropic coefficients ϵ and δ. Hence, the azimuthal variation of $x_{\min}$ can help to estimate the azimuth of the symmetry axis from 3-D converted-wave data, but it does not provide additional information about the anisotropic coefficients.

The offset $x_{\min}$ is not only responsible for the shape of the PS-wave moveout in CMP geometry, it also largely controls the asymmetry measure $\Delta \boldsymbol{x}_{PS}$ [equation (12)] defined in the slowness domain. In the symmetry-axis plane $\Delta \boldsymbol{x}_{PS}$ can be written as

$$\Delta \boldsymbol{x}_{PS} = \boldsymbol{x}_{PS}(p_1, 0) + \boldsymbol{x}_{PS}(-p_1, 0). \tag{18}$$

Linearizing equation (18) in the anisotropic coefficients using equation (8) yields the projection of the vector $\Delta \boldsymbol{x}_{PS}$ onto the x_1-axis in the form

$$(\Delta x_{PS})_{x_1} = 2\,x_0 + 12\,\eta\,z\,V_{P0}^2\,p_1^2\,\sin 4\nu\,, \tag{19}$$

where x_0 is given by equation (17). According to equation (19), the factor $|\Delta \boldsymbol{x}_{PS}|$ can be approximated by a hyperbolic function of the slowness p_1 with the value at the apex determined by $2\,x_0$. Indeed, when $p_1 = 0$, the PS-rays corresponding to both p_1 and $-p_1$ coincide and have the same offset x_0 (Figure 5). If the PS moveout were symmetric, the offsets for p_1 and $-p_1$ (circles and diamonds, respectively, in Figure 5) would have identical absolute values but *opposite* signs, and the zero-offset PS-ray would have the slowness $p_1 = 0$. Figure 5 also confirms that the linearized equation (19) is sufficiently accurate for weak and moderate anisotropy.

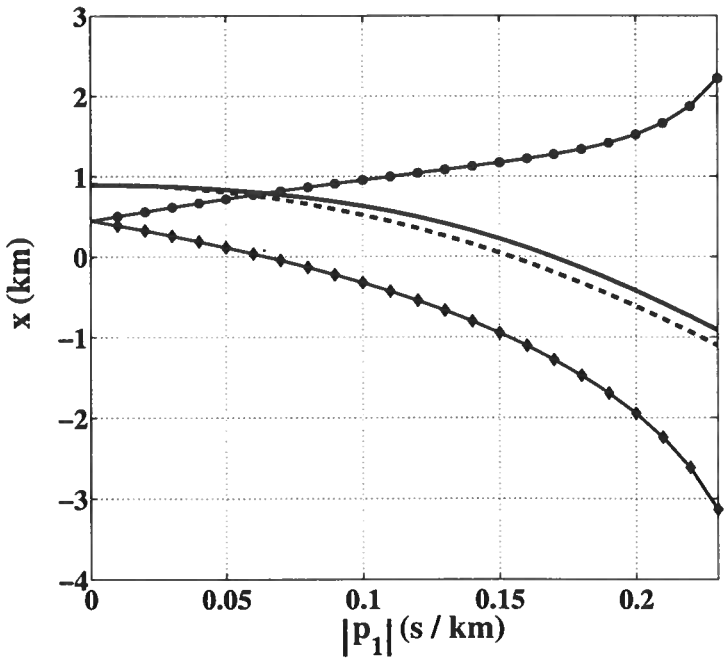

FIG. 5. Slowness-domain factor $|\Delta \boldsymbol{x}_{PS}|$ in the symmetry-axis plane of a TTI layer with the same parameters as those in Figure 2. The solid line marks exact values of $|\Delta \boldsymbol{x}_{PS}|$ from equation (18), and the dashed line is the weak-anisotropy approximation (19). Exact PS-wave offsets for positive slownesses p_1 are marked by circles, offsets for negative slownesses by diamonds; the offset is considered positive if the vector $\boldsymbol{x}_{PS}$ points in the x_1-direction.

Therefore, an alternative way of estimating x_0 is to fit a hyperbolic function to the slowness-dependent factor $|\Delta \boldsymbol{x}_{PS}|$ and find its intercept for $p_1 = 0$. It is interesting that the coefficient of the quadratic term of the hyperbola (19) is formed by the same combination of the medium parameters that governs the traveltime asymmetry factor (14).

Asymmetry factor in the offset domain.—To give an analytic description of the factor Δt_{PS} [equation (15)] in the offset domain, we expanded the traveltime in a double Taylor series around the offset $x_{\min}$ (see Appendix C). The result is convenient to represent in terms of the offset x and the azimuth α of the source-receiver line. The linearized expression (C-14) for Δt_{PS} contains linear and cubic terms in the offset x and is sufficiently accurate for relatively small offsets.

This approximation can be extended to larger offsets by adapting the approach of Tsvankin and Thomsen (1994) who developed a highly accurate nonhyperbolic moveout equation for P-waves by modifying the $t^2(x^2)$ Taylor series in such a way that it became convergent at $x \rightarrow \infty$. For long-offset converted PS-waves, the incident P-wave travels almost horizontally and accounts for most of the total reflection traveltime. The contribution of the S-leg then becomes negligible, and the asymmetry factor at infinite offset goes to zero. To ensure that Δt_{PS} vanishes for $x \rightarrow \infty$, we add a denominator $(1 + Cx^2)$ to the cubic term in equation (C-14):

$$\begin{aligned}
\Delta t_{PS} &= A\,x + \frac{B\,x^3}{1 + C\,x^2}\,; \qquad (20)\\
A &= -\frac{2\,x_0\,\cos\alpha}{z\,(V_{P0} + V_{S0})}\,,\\
B &= -\frac{4\,\eta\,V_{P0}^2\,\sin 2\nu\,\cos\alpha}{z^2\,(V_{P0} + V_{S0})^3}\left(2\cos 2\nu\,\cos^2\alpha + \sin^2\alpha\right),\\
C &= -\frac{B}{A}\,.
\end{aligned}$$

In the symmetry-axis plane ($\alpha = 0°$) the coefficients A and B in equation (20) become

$$A = -\frac{2\,x_0}{z\,(V_{P0} + V_{S0})}\,, \qquad (21)$$

$$B = -\frac{4\,\eta\,V_{P0}^2\,\sin 4\nu}{z^2\,(V_{P0} + V_{S0})^3}\,. \qquad (22)$$

The initial slope A of the asymmetry factor for the azimuth α is governed by the term $(x_0\,\cos\alpha)$ that represents the offset $x_{\min}(\alpha)$ of the local traveltime minimum [equation (16)]. The higher-order coefficient B depends on the parameter $\eta = \epsilon - \delta$ and the tilt ν, and, in principle, can be combined with A for the purpose of parameter estimation. Analysis of equation (20), however, shows that the moveout asymmetry in the offset domain can be expressed through the asymmetry factor in the slowness domain described above and the offset $x_{\min}(\alpha)$.

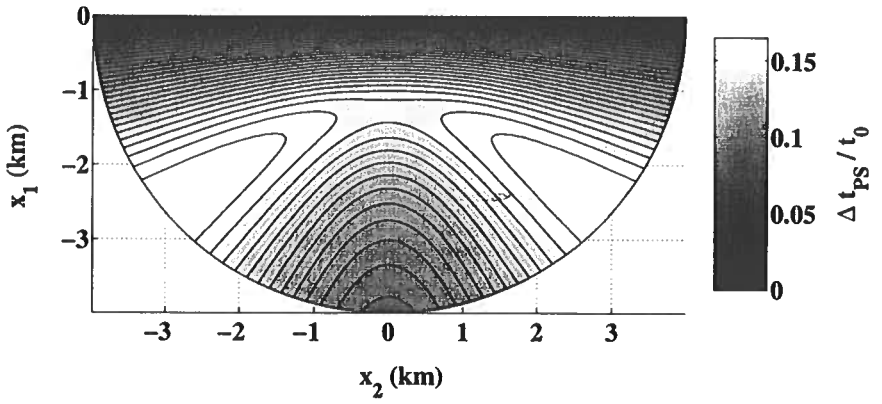

FIG. 6. Exact normalized asymmetry factor Δt_{PS} in the offset domain [equation (15)]. The data were generated by anisotropic ray tracing for the model from Figure 2. After the initial increase with offset, the asymmetry decreases for large offsets and goes to zero for $x \to \infty$.

The azimuthally varying asymmetry factor in the offset domain in Figure 6 exhibits a pattern generally similar to that of Δt_{PS} in the slowness domain. The most rapid change in Δt_{PS} is observed in the $[x_1, x_3]$-plane (see also Figure 7), while in the plane $[x_2, x_3]$ the PS-wave moveout is symmetric ($\Delta t_{PS} = 0$). The absence of the moveout asymmetry for acquisition in the x_2-direction is predicted by equation (20), which yields $\Delta t_{PS} = 0$ for $\alpha = 90°$. Note that, as discussed above, PS-waves recorded in the $[x_2, x_3]$-plane have out-of-plane slowness vectors with $p_1 \neq 0$. Therefore, the lines $x_1 = 0$ in Figure 6 and $p_1 = 0$ in Figure 2 correspond to PS arrivals with different azimuthal orientations of the source-receiver vector.

The error of the weak-anisotropy approximation (20) increases with offset before flattening out at intermediate x (Figure 7) and eventually going to zero for infinitely large offsets. Overall, equation (20) gives an adequate qualitative description of the moveout asymmetry, including a maximum in $\Delta t_{PS}(x)$ at offsets close to the reflector depth (Figure 7). By design, equation (20) also converges toward the correct value $\Delta t_{PS} = 0$ for $x \to \infty$.

PARAMETER ESTIMATION IN A TTI LAYER

The goal of the inversion algorithm introduced here is to estimate the parameters of a horizontal TTI layer from PP and PS (PSV) reflection events. As emphasized by Grechka and Tsvankin (2002) and Grechka and Dewangan (2003), effective application of the PP+PS=SS method requires acquisition of long-offset (i.e., offsets should reach at least twice the reflector depth) PP and PS data. If the offset-to-depth ratio for the recorded arrivals is less than two, the range of offsets for the constructed SS data is insufficient for obtaining a reliable estimate of the S-wave stacking velocity.

The numerical tests below prove that for a wide range of the tilt angles ν of the symmetry axis the inversion can be performed using 2-D data in the symmetry-

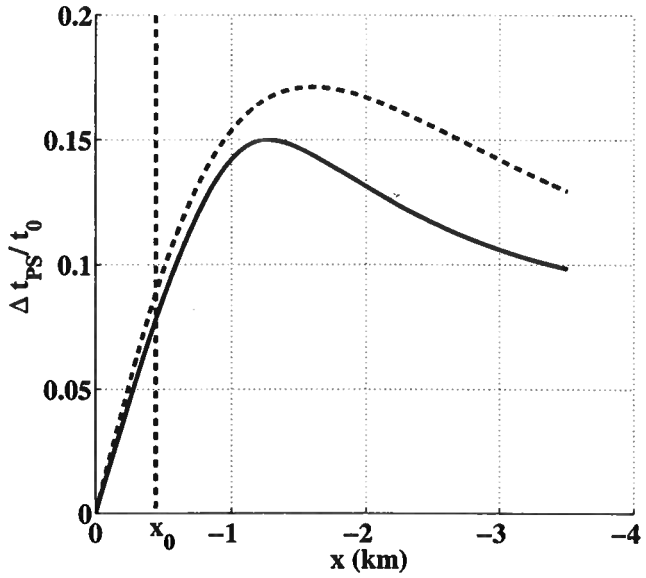

FIG. 7. Asymmetry factor from Figure 6 in the symmetry-axis plane $x_2 = 0$. The solid line is the ray-tracing result; the dashed line is the weak-anisotropy approximation (20). Also marked is the offset $x_0 = x_{\min}(\alpha = 0°)$ of the traveltime minimum.

axis plane. Full-azimuth acquisition, however, is necessary to find the orientation of this plane unless it is known, for example, from geological information. Another possible way to estimate the azimuth of the symmetry-axis plane is by analyzing the polarization direction of PS-waves at small source-receiver offsets. The azimuthal variation of reflection moveout of PP- and PS-waves is also needed to perform the inversion for TTI media with a near-horizontal orientation of the symmetry axis.

Data processing

Conventional hyperbolic velocity analysis of the PP data yields their stacking velocity ($V_{\text{nmo,P}}$) and zero-offset reflection traveltime (t_{P0}). Then, application of the PP+PS=SS method to the PP and PS records produces traces of "quasi-shear" waves that have the kinematics of the pure SS (SVSV) reflections (Grechka and Tsvankin, 2002a; Grechka and Dewangan, 2003). Therefore, processing of the constructed SS arrivals can be used to estimate the stacking velocity ($V_{\text{nmo,S}}$) and zero-offset traveltime (t_{S0}) of the SS-waves that are not physically excited in the survey. If the data have a wide range of source-receiver azimuths, azimuthal velocity analysis can be applied to obtain the NMO ellipses of the PP- and SS-waves (Grechka and Tsvankin, 1998; Grechka et al., 2002a).

The above methodology, described in detail by Grechka et al. (2002a), is designed to avoid complications associated with the processing of mode-converted waves. For some anisotropic models, the combination of PP- and SS-waves is sufficient to estimate the medium parameters without additional information. For TTI media, however, the

inversion of PP- and SS-waves is feasible only for substantial reflector dips or near-horizontal orientations of the symmetry axis (Grechka et al., 2002a).

Here, we supplement the moveouts of the PP-waves and constructed SS-waves in parameter estimation with the PS-wave asymmetry attributes obtained from the PP+PS=SS method. For laterally homogeneous media, the traveltime asymmetry $\Delta t_{PS}(x^{(3)}, x^{(4)})$ produced by the PP+PS=SS method [equation (4)] coincides the asymmetry factor defined in the slowness domain [equation (11)]. Another reason to work with the asymmetry attributes in the slowness domain is the relative simplicity of the corresponding analytic expressions.

The offset $x_{\min}(\alpha = 0)$ of the PS-wave traveltime minimum in the symmetry-axis plane $[x_1, x_3]$ can also be obtained from the PP+PS=SS method. As shown by Tsvankin and Grechka (2000) and Tsvankin (2001, Appendix 5B), the traveltime minimum of any reflected wave in CMP geometry corresponds to the ray with equal projections of the slowness vector onto the CMP line at the source and receiver locations (both legs of the ray have to be treated as upgoing waves). Applying this result to the symmetry-axis plane of a horizontal TTI layer where the slowness vector cannot have out-of-plane components, we find that the horizontal slowness at the traveltime minimum has to go to zero. Then, for both PP-waves and the constructed SS-waves the horizontal slowness has to vanish at zero offset (an obvious result for pure modes), while for PS-waves it vanishes at the offset $x_{\min}(0) = x_0$. Since the PS- and PP-waves with the same reflection point have identical absolute values of the horizontal slowness (Figure 1), the PS ray at the offset x_0 is generated by the zero-offset P-wave that corresponds to the stationary point $x_1 = x_2$.

Another way to estimate x_0 is to pick the offsets (along with the traveltimes) of the two PS-waves corresponding to the same reflection point for a range of the slownesses p_1 and build the function $|\Delta \boldsymbol{x}_{PS}(p_1)|$ [equation (18)]. This function can then be approximated with a hyperbola whose apex yields the value of x_0 [equation (19)]. The main advantage of this approach is in using multiple data points, which may help to obtain more stable estimates of x_0 for noisy data.

Inversion algorithm

We assume that the azimuth of the symmetry-axis plane was established, for example, from azimuthally varying moveout of pure modes. The general expression of the NMO ellipse has the following form (Grechka and Tsvankin, 1998):

$$V_{\rm nmo}^{-2}(\alpha) = W_{11}\cos^2\alpha + 2\,W_{12}\sin\alpha\cos\alpha + W_{22}\sin^2\alpha\,, \tag{23}$$

where $W_{ij} \equiv \tau_0\,\partial p_i/\partial x_j$ $(i,j = 1,2)$, $\tau_0 \equiv t_0/2$ is the one-way zero-offset traveltime, and p_1 and p_2 are the horizontal slowness components for one-way rays from the zero-offset reflection point to the surface; all derivatives are evaluated at the CMP location. For a homogeneous horizontal layer, the matrix $\boldsymbol{W}$ can be represented as

(Grechka et al., 1999)

$$\boldsymbol{W} = \frac{-q}{q_{,11}\,q_{,22} - q_{,12}^2} \begin{pmatrix} q_{,22} & q_{,12} \\ -q_{,12} & q_{,11} \end{pmatrix}, \tag{24}$$

where $q \equiv q(p_1, p_2)$ is the vertical slowness and $q_{,ij} \equiv \partial^2 q/(\partial p_i \partial p_j)$. As mentioned above, the slowness vector of the zero-offset ray for a horizontal layer is vertical, so the derivatives are computed for $p_1 = p_2 = 0$.

If the medium has a vertical symmetry plane, one of the axes of the NMO ellipse is parallel to the symmetry-plane direction (Grechka and Tsvankin, 1998). For a TTI layer with the symmetry axis confined to the $[x_1, x_3]$-plane, the terms $q_{,12}$ and W_{12} [equation (24)] vanish, while W_{11} and W_{22} define the semiaxes of the NMO ellipse (23). Therefore, the orientation of the NMO ellipse of the recorded PP-waves or the constructed SS-waves can be used to find the azimuth of the symmetry-axis plane $[x_1, x_3]$.

Then, as described above, the processing of 2-D multicomponent data in the symmetry-axis plane produces the following data vector $\boldsymbol{d}$:

$$\boldsymbol{d} \equiv \left\{ V_{\mathrm{nmo,P}}\,,\; t_{P0}\,,\; V_{\mathrm{nmo,S}}\,,\; t_{S0}\,,\; \Delta t_{PS}(p_1, 0)\,,\; x_{\min}(\alpha = 0^\circ) \right\}. \tag{25}$$

Although $\Delta t_{PS}(p, 0)$ denotes multiple measurements of the asymmetry factor for the available range of the horizontal slownesses p_1, equation (14) indicates that the move-out asymmetry in the $[x_1, x_3]$-plane may constrain only one combination of the layer parameters.

Analytic expressions for $\Delta t_{PS}(p_1, 0)$ and $x_0 = x_{\min}(\alpha = 0^\circ)$ needed to model these quantities in the inversion algorithm were introduced in the previous section. The NMO velocities $V_{\mathrm{nmo,P}}$ and $V_{\mathrm{nmo,S}}$ in the x_1-direction ($\alpha = 0^\circ$) can be computed from equation (24) with $q_{,12} = 0$:

$$V_{\mathrm{nmo}} = \frac{1}{\sqrt{W_{11}}} = -\frac{q}{q_{,11}}. \tag{26}$$

The model vector $\boldsymbol{m}$ includes the following parameters of the TTI layer:

$$\boldsymbol{m} \equiv \left\{ V_{P0}\,,\; V_{S0}\,,\; \epsilon\,,\; \delta\,,\; \nu,\; z \right\}. \tag{27}$$

Thus, six or more [if $\Delta t_{PS}(p_1, 0)$ constrains more than one parameter] independent measurements [equation (25)] are controlled by the six model parameters in equation (27). To estimate the vector $\boldsymbol{m}$, we applied nonlinear inversion (the Gauss-Newton method) based on exact equations for all components of the data vector (25). The misfit (objective) function minimized by the inversion algorithm is defined as

$$\begin{aligned} \mathcal{F} \;\equiv\; & w_1 \frac{(V_{\mathrm{nmo,P}}^{\mathrm{calc}} - V_{\mathrm{nmo,P}}^{\mathrm{meas}})^2}{(V_{\mathrm{nmo,P}}^{\mathrm{meas}})^2} + w_2 \frac{(V_{\mathrm{nmo,S}}^{\mathrm{calc}} - V_{\mathrm{nmo,S}}^{\mathrm{meas}})^2}{(V_{\mathrm{nmo,S}}^{\mathrm{meas}})^2} + w_3 \frac{(t_{P0}^{\mathrm{calc}} - t_{P0}^{\mathrm{meas}})^2}{(t_{P0}^{\mathrm{meas}})^2} \\ + \;& w_4 \frac{(t_{S0}^{\mathrm{calc}} - t_{S0}^{\mathrm{meas}})^2}{(t_{S0}^{\mathrm{meas}})^2} + w_5 \frac{\sum_0^p (\Delta t_{PS}^{\mathrm{calc}} - \Delta t_{PS}^{\mathrm{meas}})^2}{(\sum_0^p \Delta t_{PS}^{\mathrm{meas}})^2} + w_6 \frac{(x_0^{\mathrm{calc}} - x_0^{\mathrm{meas}})^2}{(x_0^{\mathrm{meas}})^2}, \end{aligned} \tag{28}$$

where p denotes the maximum value of the horizontal slowness p_1. The weighting coefficients w_i were generally set to unity. We observed, however, that assigning substantially larger weights to the asymmetry attributes typically leads to a faster convergence of the algorithm.

Since the exact equations for the model parameters are nonlinear and the misfit function contains local minima, selection of the starting model may have a significant influence on the performance of the algorithm. We based the initial guesses for the vertical velocities and anisotropic coefficients on the isotropic relationships,

$$V_{P0} = V_{\mathrm{nmo,P}}\,,\; V_{S0} = V_{\mathrm{nmo,S}}\,,\; \epsilon = 0,\; \delta = 0,\; z = V_{\mathrm{nmo,P}}\, t_{P0}/2\,. \tag{29}$$

Our numerical tests show that if the starting model is isotropic [equation (29)] and the initial tilt ν is set to 0° or 90°, the algorithm either does not converge toward the correct solution or the convergence is extremely slow. This happens because the initial values of the partial derivatives of the objective function (28) with respect to several model parameters go to zero. The convergence can be significantly improved by keeping the initial $\epsilon = \delta = 0$ but starting with an intermediate tilt ν that is as close as possible to the actual value. For example, if the anisotropy is known to be caused by subvertical fractures, a good choice of the initial tilt is $\nu = 70 - 80°$.

Numerical examples

We evaluated the uniqueness and stability of the inversion was evaluated by applying the algorithm to noise-contaminated input data. We analyzed a representative set of TTI models with a wide range of the tilt angles ν of the symmetry axis.

Models with tilt $\nu > 60°$.—TTI models with a significant tilt of the symmetry axis can be considered typical for dipping fracture sets because fracture planes seldom deviate far from the vertical (Angerer et al., 2002). For a system of vertical penny-shaped cracks in isotropic host rock, the symmetry axis is horizontal ($\nu = 90°$), and the medium becomes HTI.

The tilt $\nu = 70°$ of the symmetry axis in Figure 8 is quite favorable for the inversion based on the moveout asymmetry attributes of PS-waves. Here and in the other examples below, the data vector $\boldsymbol{d}$ [equation (25)] was generated using the exact equations and contaminated by Gaussian noise. The inversion was carried out for 100 realizations of the input data, which allowed us to compute the standard deviations of the estimated parameters. The initial guess was based on equation (29), with the tilt picked randomly from the interval $50° - 85°$. The model vector $\boldsymbol{m}$ [equation (27)] was estimated by minimizing the objective function specified in equation (28), as discussed in the previous section.

Figure 8 indicates that the inversion results are unbiased, and the noise is not amplified by the parameter-estimation procedure. The standard deviations are close to 0.02 for ϵ and δ, 1% for V_{P0}, 2% for V_{S0} and z, and 1° for ν. The best-constrained

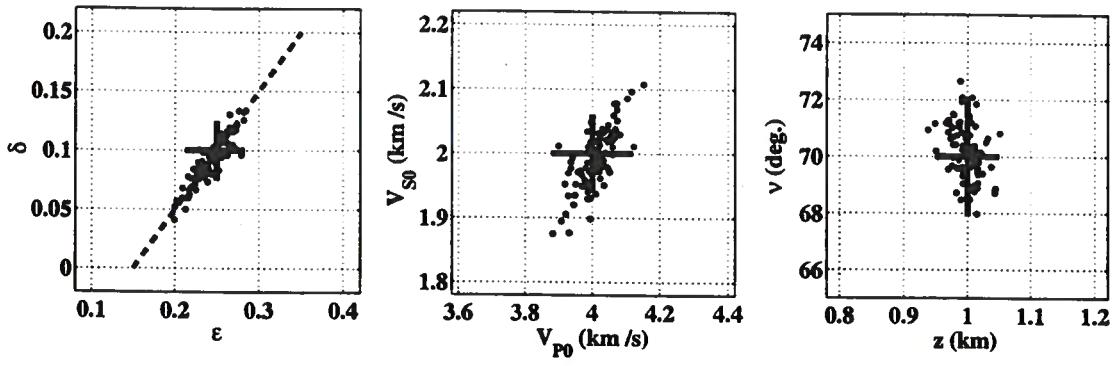

FIG. 8. Inverted parameters (dots) of a horizontal TTI layer obtained from 2-D PP and PS data in the symmetry-axis plane. The correct model parameters ($V_{P0} = 4$ km/s, $V_{S0} = 2$ km/s, $\epsilon = 0.25$, $\delta = 0.1$, $\nu = 70°$, $z = 1$ km) are marked by the crosses. The dashed line on the $[\epsilon, \delta]$ plot corresponds to the correct value of the difference $(\epsilon - \delta)$. The input data were contaminated by Gaussian noise with the standard deviations of 2% for the NMO velocities, 0.5% for the zero-offset traveltimes, and 2% for the PS-wave asymmetry attributes.

parameter combination is the difference $(\epsilon - \delta)$, which controls the asymmetry factor in the slowness domain [equations (13) and (14)] and has a strong influence on the NMO velocity of the constructed SS-waves. Although the traveltimes of the PP- and PS-waves in the symmetry-axis plane are sufficient for estimating all relevant TTI parameters, the addition of wide-azimuth data increases the accuracy of the inversion in the presence of noise.

It should be emphasized that the parameter estimation is feasible only if the asymmetry information of the PS-wave is included in the inversion algorithm. The offset x_0 of the PS-wave moveout minimum for the model from Figure 8 reaches about 1/3 of the depth z, and the asymmetry factor Δt_{PS} for the offset $x = 2z$ is about 15% of the zero-offset PS traveltime. Such a large magnitude of the traveltime asymmetry helps to constrain the tilt of the symmetry axis and the anisotropic coefficients. Without the asymmetry information the inversion becomes unstable, even if the 2-D data in the vertical symmetry plane are supplemented with the NMO ellipses of the PP- and SS-waves (Grechka and Tsvankin, 2000; Grechka et. al., 2002a).

Since the traveltime asymmetry is estimated from the relatively small difference of two time measurements, it is important to evaluate the sensitivity of the inversion results to larger errors in the PS-wave asymmetry attributes. For the test in Figure 9 the standard deviations of Δt_{PS} and x_0 were increased from 2% to 4% (also, the deviations of the zero-offset times were increased to 1%). Despite the somewhat higher scatter of the inverted parameters, the standard deviations do not exceed 0.03 for ϵ and δ, 2% for V_{P0}, 3% for V_{S0} and z, and 1° for ν. Clearly, the inversion remains sufficiently stable for realistic levels of distortions in the asymmetry attributes. In all numerical tests discussed below, the standard deviations of the noise were fixed at the values used in Figure 8.

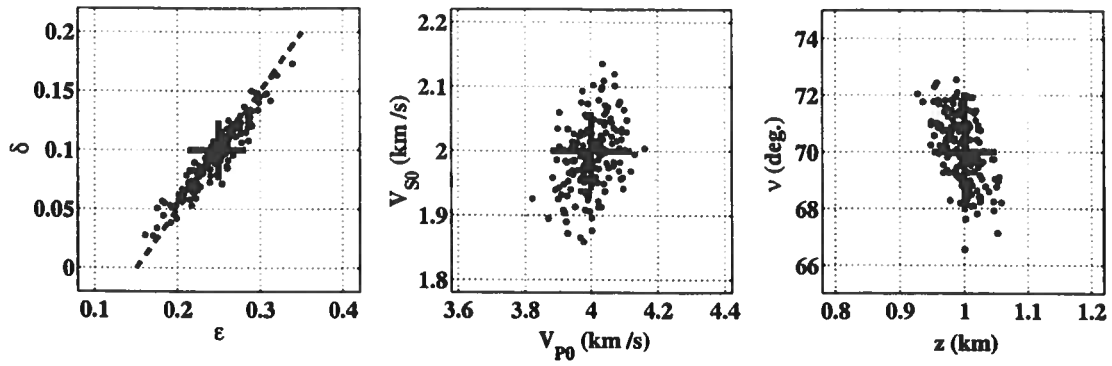

FIG. 9. Same as Figure 8, but the standard deviations of the Gaussian noise are increased to 1% for the zero-offset traveltimes and 4% for the asymmetry attributes of PS-waves (the standard deviations for the NMO velocities remain unchanged at 2%).

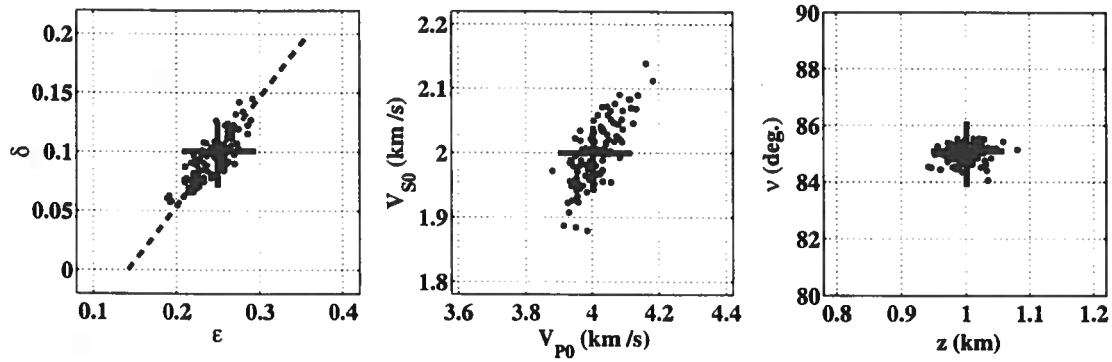

FIG. 10. Inversion results for a model with the same parameters as those in Figure 8 except for the tilt $\nu = 85°$. The standard deviations of Gaussian noise here and below are f 2% for the NMO velocities, 0.5% for the zero-offset traveltimes, and 2% for the PS-wave asymmetry attributes.

For HTI media ($\nu = 90°$) the PS-wave moveout is symmetric, and the 2-D inversion in the symmetry-axis plane cannot constrain the medium parameters. However, as illustrated by Figure 10, even a small (5°) deviation of the symmetry axis from the horizontal plane creates a measurable moveout asymmetry. For the model from Figure 10, the offset $x_{\min}$ is close to 11% of the depth z, and the factor Δt_{PS} reaches about 4% of the zero-offset PS traveltime for $x = 2z$. Although the magnitude of the asymmetry attributes is not large, it proved to be sufficient for stable 2-D parameter estimation. The standard deviations do not exceed 0.02 for ϵ and δ, 2% for V_{P0}, V_{S0}, and z, and 1° for ν.

Models with intermediate tilt.—The moveout asymmetry factor in the slowness domain is small not only for near-vertical and near-horizontal orientations of the symmetry axis, but also for tilts ν close to 45° [equation (14)]. The model of a

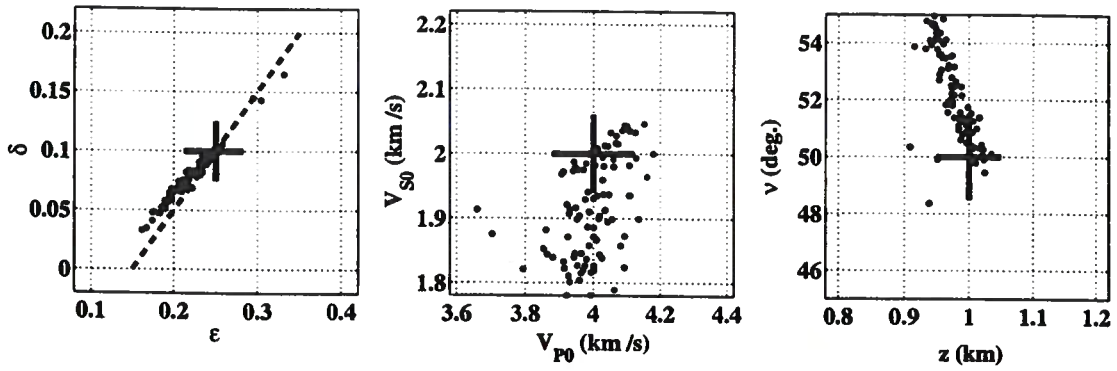

FIG. 11. Inversion results for a model with the same parameters as those in Figure 8 except for the tilt $\nu = 50°$.

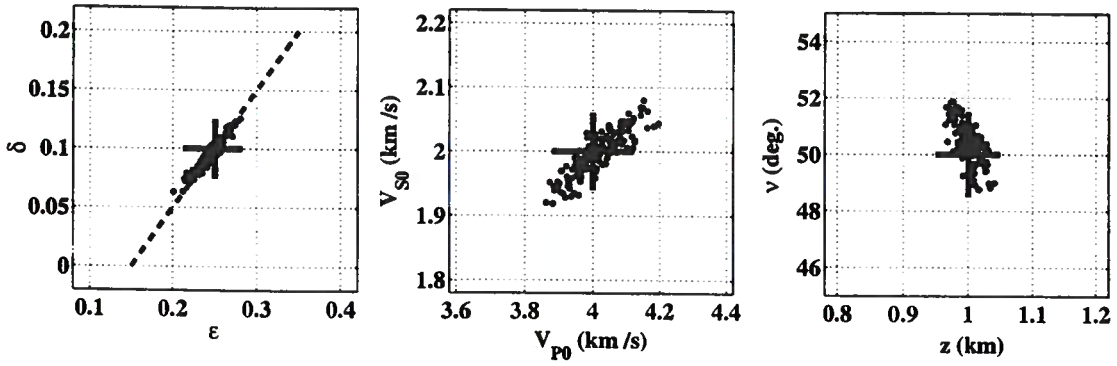

FIG. 12. Same as Figure 11, but the inversion algorithm is modified to avoid local minima.

horizontal TTI layer with $35° < \nu < 55°$ can be used to describe reflections from a horizontal interface beneath dipping shale layers in fold-and-thrust belts, such as the Canadian Foothills (e.g., Isaac and Lawton, 1999).

Figure 11 helps to assess the feasibility of the inversion for a tilt of 50°. Although the asymmetry in the offset domain for intermediate tilts is substantial (x_0 is about 34% of z), the inverted parameters are biased and exhibit significant scatter. Analysis of the inversion results shows that many estimated models correspond to local minima of the objective (misfit) function and do not fit the input data within the noise level.

The problem with local minima was addressed by modifying the inversion algorithm. If the search stops at a minimum where the model does not fit the data within the standard deviation of the noise (2% for the NMO velocities and the asymmetry attributes and 0.5% for the zero-offset traveltimes), then the model is perturbed to resume the search from a different point in the parameter space. Figure 12 shows that if the algorithm does not get trapped in local minima, the inversion results for $\nu = 50°$ become quite stable, with the standard deviations comparable to those for $\nu = 70°$ (Figure 8).

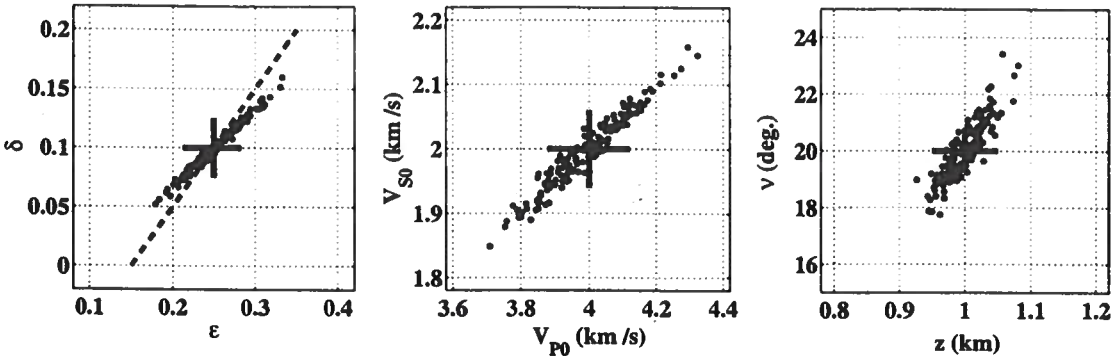

FIG. 13. Inversion results for a model with the same parameters as those in Figure 8 except for the tilt $\nu = 20°$.

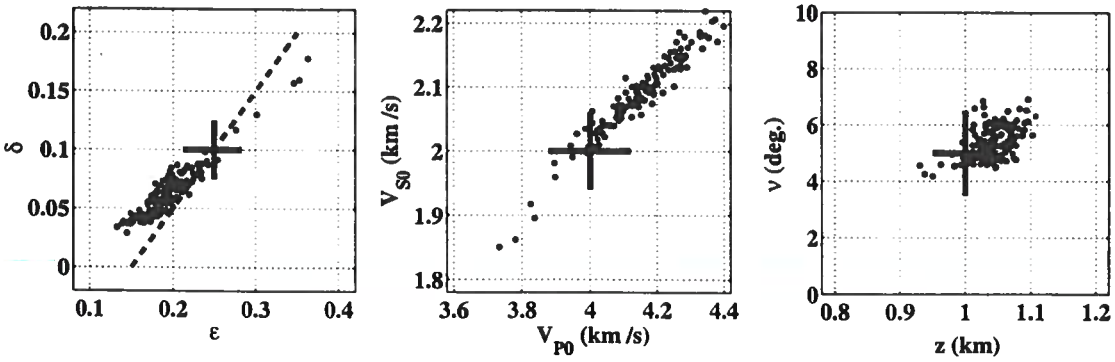

FIG. 14. Inversion results for a model with the same parameters as those in Figure 8 except for the tilt $\nu = 5°$.

Models with mild tilt.—For completeness, here we discuss the parameter-estimation results for mild tilts ν. While such models are not plausible if the anisotropy is caused by dipping fractures, they may be adequate for effective TTI models formed by progradational sequences (e.g., Sarg and Schuelke, 2003).

The scatter in the inversion results for a tilt of 20° is slightly higher than that for large tilts, but the standard deviations are less than 0.03 for ϵ and δ, 3% for V_{P0}, V_{S0} and z, and 2° for ν (Figure 13). As expected, the parameter estimation breaks down as the model approaches VTI, and the tilt ν becomes smaller than 10°. Not only do the standard deviations rapidly increase when $\nu \to 0°$, but the parameter estimates become noticeably biased. For the model with $\nu = 5°$ in Figure 14, the bias is about 0.05 for ϵ, 0.03 for δ, and 4% for V_{P0}, V_{S0}, and z. Only the tilt is relatively well-constrained by the data because of the sensitivity of the asymmetry attributes to ν.

Elliptically anisotropic models.—According to our analytic results, the move-out asymmetry of PS-waves in the slowness domain vanishes if the medium is ellipti-

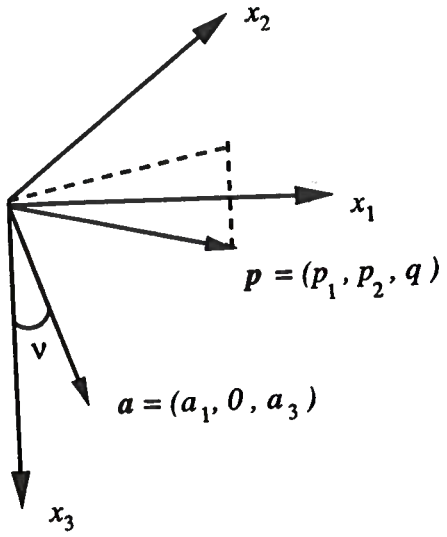

FIG. A-1. The symmetry axis is defined by the unit vector $\boldsymbol{a}$ confined to the $[x_1, x_3]$-plane. The slowness vector $\boldsymbol{p}$ has an arbitrary orientation.

APPENDIX A: APPROXIMATE MOVEOUT ASYMMETRY FACTOR IN THE SLOWNESS DOMAIN

For a weakly anisotropic TTI layer ($|\epsilon| \ll 1$ and $|\delta| \ll 1$), the asymmetry factor Δt_{PS} in the slowness domain [equations (11) and (5)] can be linearized in the anisotropic coefficients ϵ and δ. Without losing generality, the symmetry axis (unit vector $\boldsymbol{a}$) is assumed to lie in the coordinate plane $[x_1, x_3]$ (Figure A-1):

$$\boldsymbol{a} \equiv [a_1, 0, a_3] = [\sin\nu, 0, \cos\nu]\,, \tag{A-1}$$

where ν is the tilt of the symmetry axis from the vertical direction.

To obtain the vertical slowness q as a function of the horizontal slowness components p_1 and p_2 for both legs of the PS reflected ray, we use the approach suggested by Grechka and Tsvankin (2000, Appendix B). The component q can be represented as the sum of the isotropic value $\tilde{q}$ and the anisotropy-induced correction term Δq:

$$q \equiv p_3 = \tilde{q} + \Delta q\,. \tag{A-2}$$

For P-waves in an isotropic medium with the velocity V_{P0}, the vertical slowness is given by

$$\tilde{q} = \sqrt{\frac{1}{V_{P0}^2} - p_1^2 - p_2^2}\,. \tag{A-3}$$

In the weak-anisotropy approximation Δq can be treated as the linear term in a Taylor series expansion of q in ϵ and δ for fixed horizontal slownesses p_1 and p_2:

$$\Delta q = -\frac{1}{\partial\mathcal{F}/\partial q}\left(\frac{\partial\mathcal{F}}{\partial\epsilon}\,\epsilon + \frac{\partial\mathcal{F}}{\partial\delta}\,\delta\right), \tag{A-4}$$

where $\mathcal{F}(q, p_1, p_2, V_{P0}, V_{S0}, \epsilon, \delta, \nu) = 0$ is the Christoffel equation for P- and SV-waves in TTI media.

Next, we obtain the partial derivatives $q_{,i} \equiv \partial q/\partial p_i$ $(i = 1, 2)$ for the P-wave, substitute them into equations (7) and then (11), and carry out further linearization using symbolic software Mathematica. The weak-anisotropy approximation for the contribution of the P-leg of the PS-wave to the asymmetry factor has the form

$$\Delta t_P = 4\, z\, (\delta - \epsilon)\, p_1 V_{P0}^2 \sin 2\nu \left[p_2^2 + (2p_1^2 + p_2^2) \cos 2\nu\right]. \qquad \text{(A-5)}$$

The linearized asymmetry contribution of the S-leg can be found from the P-wave equation (A-5) by using the following general transformation rule (Tsvankin, 2001, p. 26):

$$V_{P0} \rightarrow V_{S0},\ \epsilon \rightarrow 0,\ \delta \rightarrow \sigma\,;$$

$$\sigma \equiv \frac{V_{P0}^2}{V_{S0}^2}\,(\epsilon - \delta)\,.$$

Taking into account that the asymmetry for the S-leg of a given PS-ray has to be computed for the opposite sign of the horizontal slowness [so p_1 in equation (A-5) has to be replaced with $-p_1$, and p_2 with $-p_2$], we find

$$\Delta t_S = -4\, z\, (\epsilon - \delta)\, p_1 V_{P0}^2 \sin 2\nu \left[p_2^2 + (2p_1^2 + p_2^2) \cos 2\nu\right] = \Delta t_P\,. \qquad \text{(A-6)}$$

APPENDIX B: AZIMUTHAL VARIATION OF THE OFFSET X_{MIN}

The slope dt/dx of the CMP moveout curve for any pure or converted reflection mode is determined by the difference between the projections onto the CMP line of the slowness vectors at the source and receiver locations[2] (Tsvankin and Grechka, 2000; Tsvankin, 2001, Appendix 5B). This general result, which is valid for any heterogeneous, anisotropic medium, can be used to find the offset $x_{\min}$ of the PS-wave traveltime minimum where the moveout slope goes to zero. For a horizontal, laterally homogeneous layer, the horizontal slowness has the same absolute value for both legs of the reflected ray, and the slope can vanish only for a ray with the slowness vector orthogonal to the CMP line.

Suppose p_α is the projection of the slowness vector onto the CMP line that makes the angle α with the x_1-axis, and p_t is the slowness projection onto the orthogonal $(\alpha + 90^\circ)$ direction. The offset $x_{\min}(\alpha)$ then corresponds to the PS ray for which $p_\alpha = 0$. Rotating the slowness vector by the angle α in the horizontal plane yields

$$p_1 = p_\alpha \cos\alpha - p_t \sin\alpha\,, \qquad \text{(B-1)}$$

$$p_2 = p_\alpha \sin\alpha + p_t \cos\alpha\,. \qquad \text{(B-2)}$$

[2] In this formulation both legs of the reflected ray are treated as upgoing waves.

The offset x can be parametrically represented as [equations (8) and (9)]

$$x = z\sqrt{(q_{,1P} - q_{,1S})^2 + (q_{,2P} - q_{,2S})^2}\,. \tag{B-3}$$

To find $x_{\min}$ from equation (B-3), the derivatives $q_{,i} \equiv \partial q/\partial p_i$ $(i = 1, 2)$, which are derived for weakly anisotropic TTI media in Appendix A, have to be evaluated for $p_\alpha = 0$.

Substituting $q_{,i}$ from Appendix A into equation (B-3) and further linearizing the result in ϵ and δ produces x as a function of p_1 and p_2, which can be replaced by p_α and p_t using equations (B-1) and (B-2). The component p_α is then set to zero, while p_t can be found from equation (10) for the azimuth α. Linearizing equation (10) and using equations (B-1) and (B-2) with $p_\alpha = 0$ allows us to obtain p_t:

$$p_t = \frac{x_0 \sin\alpha}{V_{S0} - V_{P0}}\,, \tag{B-4}$$

where $x_0 = x_{\min}(\alpha = 0°)$ is the value of $x_{\min}$ in the symmetry-axis plane.

Since the slowness vectors of reflected rays propagating in the symmetry-axis plane cannot have out-of-plane components, the offset x_0 corresponds to the ray with the vertical slowness vector ($p_\alpha = p_t = p_1 = p_2 = 0$). Evaluating x from equation (B-3) with $p_1 = p_2 = 0$ gives

$$x_0 = z\left[\epsilon \sin 2\nu - \frac{1}{2}(\epsilon - \delta)\left(1 + \frac{V_{P0}^2}{V_{S0}^2}\right)\sin 4\nu\right]. \tag{B-5}$$

Finally, we substitute $p_\alpha = 0$ and p_t from equations (B-4) and (B-5) into equation (B-3) to obtain the following expression for the azimuthally varying offset of the moveout minimum:

$$x_{\min}(\alpha) = x_0 \cos\alpha\,. \tag{B-6}$$

APPENDIX C: APPROXIMATE MOVEOUT ASYMMETRY FACTOR IN THE OFFSET DOMAIN

To describe the moveout asymmetry in the offset domain defined in equation (15), we express the PS traveltime through the components x_1 and x_2 of the PS-wave offset vector $\boldsymbol{x}_{PS}$ [equation (8)]. An approximation for the asymmetry factor in a horizontal TTI layer can be found by expanding the traveltime $t(x_1, x_2)$ in a double Taylor series in the vicinity of the offset $(x_0, 0)$ of the moveout minimum [equation (B-5)]:

$$\begin{aligned} t(x_1, x_2) &= t(x_0, 0) + \frac{\partial t}{\partial x_1}(x_1 - x_0) + \frac{\partial t}{\partial x_2}x_2 \\ &+ \frac{1}{2}\frac{\partial^2 t}{\partial x_1^2}(x_1 - x_0)^2 + \frac{1}{2}\frac{\partial^2 t}{\partial x_2^2}x_2^2 + \frac{\partial^2 t}{\partial x_1 \partial x_2}(x_1 - x_0)\,x_2 \\ &+ \frac{1}{3!}\frac{\partial^3 t}{\partial x_1^3}(x_1 - x_0)^3 + \frac{1}{3!}\frac{\partial^3 t}{\partial x_2^3}x_2^3 \\ &+ \frac{1}{2}\frac{\partial^3 t}{\partial x_1^2 \partial x_2}(x_1 - x_0)^2\,x_2 + \frac{1}{2}\frac{\partial^3 t}{\partial x_1 \partial x_2^2}(x_1 - x_0)\,x_2^2 + \ldots\,. \end{aligned} \tag{C-1}$$

The traveltime derivatives in equation (C-1) should be evaluated at ($x_1 = x_0$, $x_2 = 0$). Note that the first derivatives $\partial t/\partial x_1$ and $\partial t/\partial x_2$ at $(x_0, 0)$ are equal to zero.

The moveout asymmetry factor in the offset domain can be found from equation (C-1) as

$$\begin{aligned}\Delta t_{PS}(x_1, x_2) &= t_{PS}(x_1, x_2) - t_{PS}(-x_1, -x_2) \\ &= -2\frac{\partial^2 t}{\partial x_1^2} x_1 x_0 - 2\frac{\partial^2 t}{\partial x_1 \partial x_2} x_2 x_0 + \frac{1}{3}\frac{\partial^3 t}{\partial x_1^3}(x_1^3 + 3x_1 x_0^2) \\ &+ x_2\left[\frac{\partial^3 t}{\partial x_1^2 \partial x_2}(x_0^2 + x_1^2) + \frac{\partial^3 t}{\partial x_1 \partial x_2^2} x_1 x_2 + \frac{1}{3}\frac{\partial^3 t}{\partial x_2^3} x_2^2\right]. \qquad \text{(C-2)}\end{aligned}$$

Since $[x_1, x_3]$ is a plane of symmetry, $\Delta t_{PS}(x_1, x_2)$ has to be an even function of x_2:

$$\Delta t_{PS}(x_1, x_2) = \Delta t_{PS}(x_1, -x_2)\,. \qquad \text{(C-3)}$$

Therefore, equation (C-2) should not contain terms linear and cubic in x_2, and

$$\frac{\partial^2 t}{\partial x_1 \partial x_2} = \frac{\partial^3 t}{\partial x_1^2 \partial x_2} = \frac{\partial^3 t}{\partial x_2^3} = 0\,. \qquad \text{(C-4)}$$

The second- and third-order derivatives in equation (C-2) are convenient to represent in terms of the slowness components of the ray with $p_1 = p_2 = 0$ that corresponds to the offset x_0 (see Appendix B). The time slopes $\partial t/\partial x_i$ $(i = 1, 2)$ can be expressed through the the horizontal slownesses p_1 and p_2 of the PS-wave using the results of Tsvankin (2001, Appendix 5B):

$$\frac{\partial t}{\partial x_i} = -p_i\,(i = 1, 2)\,. \qquad \text{(C-5)}$$

Differentiating $\partial t/\partial x_1$ from equation (C-5) with respect to x_1 and using equation (8) yields

$$\frac{\partial^2 t}{\partial x_1^2} = \frac{\partial}{\partial x_1}\frac{\partial t}{\partial x_1} = \frac{-1}{\partial x_1/\partial p_1} = \frac{-1}{z\,(q_{,1P,1P} - q_{,1S,1S})}\,, \qquad \text{(C-6)}$$

where $q_{,jP,iP} \equiv \partial^2 q_P/(\partial p_j \partial p_i)$ and $q_{,jS,iS} \equiv \partial^2 q_S/(\partial p_j \partial p_i)$.

The third-order derivatives of the traveltime t needed in equation (C-2) can be obtained in a similar fashion:

$$\begin{aligned}\frac{\partial^3 t}{\partial x_1^3} &= \frac{\partial}{\partial x_1}\left(\frac{-1}{\partial x_1/\partial p_1}\right) = \frac{\partial}{\partial p_1}\left(\frac{-1}{\partial x_1/\partial p_1}\right)\left(\frac{\partial p_1}{\partial x_1}\right) \\ &+ \frac{\partial}{\partial p_2}\left(\frac{-1}{\partial x_1/\partial p_1}\right)\left(\frac{\partial p_2}{\partial x_1}\right) = \frac{q_{,1P,1P,1P} - q_{,1S,1S,1S}}{z^2\,(q_{,1P,1P} - q_{,1S,1S})^3}\,, \qquad \text{(C-7)}\end{aligned}$$

$$\frac{\partial^3 t}{\partial x_1 \partial x_2^2} = \frac{\partial}{\partial x_1}\left(\frac{-1}{\partial x_2/\partial p_2}\right) = \frac{\partial}{\partial p_1}\left(\frac{-1}{\partial x_2/\partial p_2}\right)\left(\frac{\partial p_1}{\partial x_1}\right) + \frac{\partial}{\partial p_2}\left(\frac{-1}{\partial x_2/\partial p_2}\right)\left(\frac{\partial p_2}{\partial x_1}\right) = \frac{q_{,2P,2P,1P} - q_{,2S,2S,1S}}{z^2\,(q_{,2P,2P} - q_{,2S,2S})^2\,(q_{,1P,1P} - q_{,1S,1S})}. \tag{C-8}$$

Here $q_{,jP,iP,kP} \equiv \partial^3 q_P/(\partial p_j \partial p_i \partial p_k)$, $q_{,jS,iS,kS} \equiv \partial^3 q_S/(\partial p_j \partial p_i \partial p_k)$, and the derivative $(\partial p_2/\partial x_1)$ vanishes because $p_2 = 0$ on the x_1-axis.

Using the linearized derivatives of the vertical slowness q [equation (A-2)] from Appendix A leads to

$$\frac{\partial^2 t}{\partial x_1^2} = \frac{2}{z}\left\{V_{P0}\,[2 + \delta + \epsilon + 2\epsilon\cos 2\nu + 3(\delta - \epsilon)\cos 4\nu] \right. \tag{C-9}$$

$$\left. + \; V_{S0}\,(2 + \sigma + 3\sigma\cos 4\nu)\right\}^{-1}, \tag{C-10}$$

$$\frac{\partial^3 t}{\partial x_1^3} = -\frac{12(\epsilon - \delta)\,V_{P0}^2 \sin 4\nu}{z^2\,(V_{P0} + V_{S0})^3}, \tag{C-11}$$

$$\frac{\partial^3 t}{\partial x_1 \partial x_2^2} = -\frac{4(\epsilon - \delta)\,V_{P0}^2 \sin 2\nu}{z^2\,(V_{P0} + V_{S0})^3}. \tag{C-12}$$

Substituting equations (C-9)–(C-12) into equation (C-2) and further linearizing the result, we obtain the asymmetry factor as

$$\Delta t_{PS} = -\frac{2\,x_1\,x_0}{z\,(V_{P0} + V_{S0})} - \frac{4(\epsilon - \delta)\,V_{P0}^2 \sin 4\nu}{z^2\,(V_{P0} + V_{S0})^3}\,x_1^3 - \frac{4(\epsilon - \delta)\,V_{P0}^2 \sin 2\nu}{z^2\,(V_{P0} + V_{S0})^3}\,x_1\,x_2^2. \tag{C-13}$$

Finally, equation (C-13) can be rewritten in terms of the offset x and the azimuth α of the source-receiver line ($x_1 = x\cos\alpha$, $x_2 = x\sin\alpha$):

$$\Delta t_{PS}(x,\alpha) = -\frac{2\,x\,x_0\cos\alpha}{z\,(V_{P0} + V_{S0})} - \frac{4(\epsilon - \delta)\,V_{P0}^2 \sin 4\nu}{z^2\,(V_{P0} + V_{S0})^3}\,x^3\cos^3\alpha - \frac{4(\epsilon - \delta)\,V_{P0}^2 \sin 2\nu}{z^2\,(V_{P0} + V_{S0})^3}\,x^3\cos\alpha\sin^2\alpha,$$

or

$$\Delta t_{PS}(x,\alpha) = -\frac{2\,x\,x_0\cos\alpha}{z\,(V_{P0} + V_{S0})} - \frac{4\,x^3(\epsilon - \delta)\,V_{P0}^2 \sin 2\nu\cos\alpha}{z^2\,(V_{P0} + V_{S0})^3}\left(2\cos 2\nu\cos^2\alpha + \sin^2\alpha\right). \tag{C-14}$$